Flexible AlScN based PMUT arrays for conformal and wearable ultrasound

Epimitheas Georgitzikis, Pieter Gijsenbergh, Gianluca Massimino, Robert Ukropec, Milind Pandit, Jeremy Segers, Dominika Wysocka, Denis Van Lancker, Zhiyuan Shen, Grim Keulemans, Paresh Limaye, Erwin Hijzen
imec, Kapeldreef 75, 3001 Leuven
Email: Epimitheas.Georgitzikis@imec.be

***Abstract*— Flexible transducers address the limitations of conventional rigid ultrasound probes for wearable applications, such as the continuous monitoring of vital organs. In this work, we demonstrate the first flexible micromachined ultrasound transducer array based on AlScN piezoelectric film. Using flat-panel display compatible technology which enables the manufacturing of large-aperture arrays we demonstrate a piezoelectric transducer with an active area of 1.5x1.5 cm^2. The rigid glass substrate is removed and replaced by a flexible acoustic backing layer. Optimizations on thickness, mechanical rigidity, and acoustic properties of the backing material were performed to maximize the flexible transducer performance leading to transmit sensitivity of 3.8 kPa/V at 1.8 MHz and capable of acoustic imaging functionalities.**

***Keywords*— PMUT, ultrasound, acoustics, conformal, wearable, imaging, microfabrication, characterization, flexible**

I. Introduction

Following the advances in ultrasound technology, from bulk piezoceramics via the introduction of microfabrication to piezoelectric micromachined ultrasound transducers (PMUT), the application space of ultrasound devices has broadened beyond the well-established domains such as echography [1], park assistance sensors and flow meters [2]. Emerging applications include wearable ultrasound patches, touchless gesture recognition [3], mid-air haptic feedback [4], [5], and human-machine interfacing [6]. Several of these new application fields require for the transducer to extend to large area form factors covering several cm^2 of aperture area and to become flexible in order to conform to different shapes and types of surfaces, such as a human body, a car window screen or a robotic arm [7], [8]. The commercially available PMUT arrays cannot address these requirements, as they are fabricated on rigid silicon wafers with footprints that do not exceed 0.5×0.5 cm^2 [9].

Flexible ultrasound transducers can overcome the described limitations, enabling devices such as wearables for the continuous monitoring of vital organs [10]. Previous approaches towards flexible transducers include piezocomposites with stretchable matrix [11], organic piezoelectric materials like polyvinylidene [12] or spring-shaped silicon hinges in between MUT subarrays or integrating these subarrays on an elastic substrate [13], [14]. Whilst these approaches have been successful in manufacturing small patch-like transducers, their process is inherently not compatible with large-area patches that are crucial for medical imaging of large body organs such as the heart, bladder, and lungs. This work presents the first flexible micromachined ultrasound transducer (MUT) array based on AlScN piezoelectric film continuing from our previous work [15]. Using flat-panel technology, volume manufacturing of flexible and large-aperture arrays is enabled with sufficient acoustic performance for medical imaging applications. Here we demonstrate an array with an active area of 1.5 cm x 1.5 cm (Fig. 1).

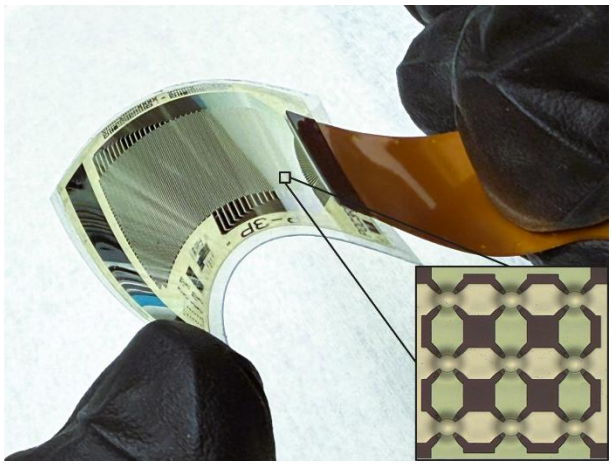

Fig. 1. Flexible 32x32 pixel PMUT array with micrograph view on a single pixel containing 3x3 PMUT.

II. Flexible PMUT Technology

For the PMUT technology, a flat-panel compatible process flow is developed, following our previously reported approach [16]. The frontplane stack is formed by growing a 500 nm thick $Al_{0.7}Sc_{0.3}N$ piezoelectric on a 150-mm glass wafer coated with a polyimide layer, which will serve as the flexible transducer membrane. Above and underneath the AlScN, metals are patterned to create electrodes and interconnects. A secondary glass wafer is coated with polyimide to serve as a temporary carrier, onto which the frontplane stack will be

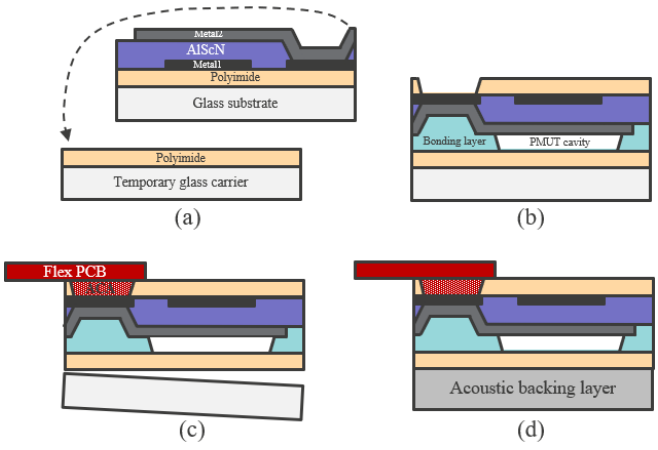

Fig. 2. (a) Frontplane stack and temporary carrier, (b) Bonding via pattern intermediate layer, and polyimide etch after glass LLO, (c) Connector attachment and carrier glass LLO, (d) ABL application.

flipped, as shown in Fig. 2(a). Bonding between the two substrates is achieved via an intermediate photo-patternable adhesive photoresist, which is patterned to form PMUT cavities of 35 µm radius and pitch of 120 µm. Following the bonding step, the original glass substrate is removed via laser lift-off (LLO) with an excimer laser debonder (ELD3000) and the exposed polyimide is etched to reveal the metal contact pads. This step is depicted in Fig. 2(b). At this point, the wafer is diced into single transducer arrays. This process provides complete design flexibility towards array size and form factor and can be upscaled to larger wafer sizes or panels. At die level, a flexible interconnect PCB is bonded to the PMUT array using anisotropically conductive adhesive (ACA). The glass carrier wafer is removed using another LLO step, as summarized in Fig. 2(c). Finally, the acoustic backing layer is bonded to the stack and trimmed to size to achieve the outcome on Fig. 2(d) and Fig. 1.

III. Transducer Design and Simulation

A. 3D single cell PMUT model

In the case of a device working in plane wave condition, all the transducers are driven contemporary by the same signal. A 3D single cell PMUT multiphysics model, with periodic symmetry conditions on the vertical lateral surfaces, is created to capture the local near-field behaviour. The PMUT cavity is cylindrical with a radius R_{PMUT} = 35 µm the pitch is equal to 120 µm. The bottom and top electrode are coaxial with the PMUT and their radius is R_{elec} = 23 µm as presented in Fig. 3 (a). The numerical model is characterized by a set of fully coupled physics, i.e., elastodynamics in the layered system, electrostatics in the piezoelectric layer and pressure acoustics in the water domain [17]. Fabrication induced residual stresses are taken into account by means of a measured initial amount of stress. Proper structural and dielectric losses are considered in the transducer's layers [18]. The Acoustic-Structure Interaction (ASI) condition is enforced on the device wet surface. The acoustic domain has a height of 4λ, where λ = 592 µm is the wavelength at 2.5 MHz. An acoustic Absorbing Boundary Condition (ABC) is applied on its top surface to simulate the wave transmission in an infinite medium. The Stokes' sound attenuation law is implemented in the water domain. A perturbated frequency sweep study is carried out in the range [1 MHz, 4 MHz], under a harmonic voltage difference of 1 V AC. Hence, the surface average normal acceleration is calculated over the PMUT footprint.

B. 3D PMUT array model

The response of the actual sized device is calculated at the natural focus, which is 13 cm far from the PMUT array surface, by means of an additional FEM model. It consists of a pressure acoustics cylindrical domain. Only one eighth of the system is modelled, as reported in Fig. 3 (b) and symmetry is exploited. The domain has a radius equal to 12.2 cm and a height of 2λ where a λ thick PML domain is considered to simulate the pressure emission into an infinite medium. The transducers are modelled by means of the equivalent vibrating baffled pistons [19] where the previously computed average normal acceleration is enforced at each PMUT sites. To solve the acoustic problem, a frequency sweep analysis is carried out in the range [1 MHz,

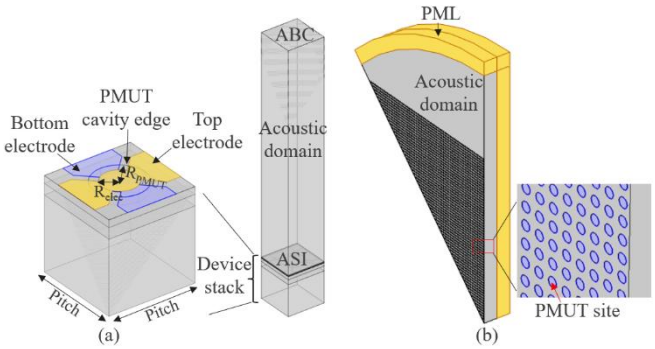

Fig. 3. Multiphysics numerical models. (a) Single PMUT with domain description, top electrode highlighted in yellow and bottom electrode in blue. (b) PMUT array with domain description, PML in highlighted yellow and PMUT in blue.

4 MHz]. To compute the transmit sensitivity at the natural focus, the Kirchhoff–Helmholtz integral technique is used. Considering both cases of rigid and flexible device, the obtained numerical results are reported in Fig. 7 together with the corresponding measured ones. Note that the described numerical modelling strategy correctly captures the experimental observations.

IV. Transducer Characterization

An assessment of the electrical, mechanical and acoustical properties of the ultrasound transducer arrays is conducted. The performance across these three domains is compared between a fully flexible PMUT matrix and an array still on its glass carrier.

A. Electrical impedance and electromechanical coupling

The electrical impedance and phase in function of the applied frequency were measured on rigid and flexible PMUT arrays using a Keysight E4990A impedance analyzer. As shown in Fig. 4, the phase peak of the flexible array in air occurs around 3.15 MHz, approximately 7% lower than the peak frequency of 3.4 MHz for the rigid sample. The peak prominence on ABL is also reduced, indicating increased energy dissipation, due to a combination higher mechanical damping due to the polymeric backing and increased electrical resistivity. The latter effect is also supported by the increase in phase values, further away from the pure capacitor at -90º, and can be linked to the interconnection between the PMUT matrix and the flex PCB.

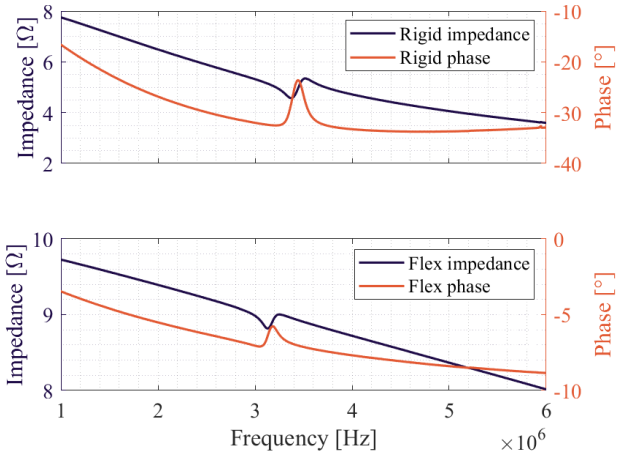

Fig. 4. Impedance and phase spectrum for PMUT matrix on glass (top) and on flexible ABL (bottom).

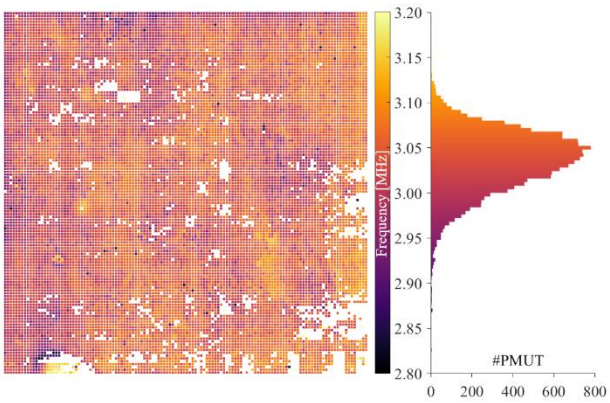

Fig. 5. Resonance frequency map and histogram for flexible 32x32 array of 4x4 PMUT pixels. Devices that are not responsive (i.e. no resonance peak is detected) are left blank.

The electromechanical coupling coefficient (EMCC) $k^2_{eff} = (f^2_a - f^2_r) / f^2_r$ describing the transduction efficiency was obtained from the resonant (f_r) and anti-resonant (f_a) frequencies, across a dozen samples of each variant [20]. With an average k_{eff} around 0.27 for both the rigid and the flex samples, it can be concluded that transferring the PMUT transducers to a flexible ABL does not directly lead to any reduction in EMCC, albeit at a lower operating frequency and with somewhat increased dissipation.

B. *Mechanical parameters*

A Polytec laser Doppler vibrometer type MSA-500 is used to mechanically characterize all individual PMUT in a rigid and a flexible array in air. A frequency sweep from 1 kHz to 10 MHz is applied to all PMUT simultaneously using an arbitrary waveform generator and the mechanical displacement of each membrane center is measured. A map of the center frequency for all PMUT of the flexible array is shown in Fig. 5, alongside a 100-bin histogram showing slight asymmetry towards the lower range of the span. In the entire 32-row, 32-column matrix of 4-by-4 PMUT, 1242 membranes are determined to be unresponsive. I.e. due to mechanical or electrical failure – likely originating in the last fabrication step – no peak in the frequency response is found. As such, the total yield is calculated to be 92.41%. On glass, prior to ABL application, only 3 of nearly 17000 PMUT fail.

The key mechanical characteristics are summarized in Table 1 and align closely with the electrical measurement results. The stricter clamping conditions of the devices still on glass result in a higher f_c and tighter spread (lower σ_f). Averaging the mechanical response over all elements, yields the graph shown in Fig. 6. Actuating an array at its center frequency in air induces an average membrane center displacement of 15.1 nm/V for the rigid array and 4.8 nm/V for the flexible array.

TABLE I. Comparison of mechanical characteristics.

	RIGID	FLEX
Center frequency f_c	3.38 MHz	3.04 MHz
Standard deviation σ_f	31.6 kHz	39.4 kHz
Bandwidth BW	124.2 kHz	154.3 kHz
Mean deflection d_{avg}	15.1 nm/V	4.75 nm/V
Process yield Y	99.98%	92.41%

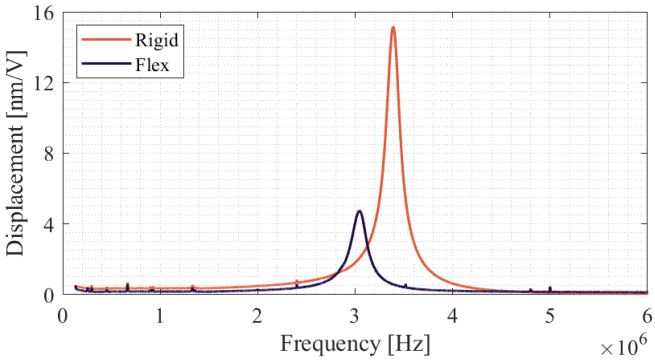

Fig. 6. Overall array frequency response, averaged over all PMUT. In air, the fractional bandwidth of the flexible system is 5.1%, while for the rigid system this is 3.7%.

Although the average mechanical output of the flexible array is approximately three times lower than that of its rigid counterpart, it should be noted that in both cases, a preponderance of PMUT is actuated off-resonance. The cited mean displacements in fact represent a 44.7% and a 17.8% array efficiency for the rigid and flex versions respectively. i.e., at the respective center frequencies, the champion performers in these arrays reach 33.8 nm/V and 26.7 nm/V. Two of the major contributors to the lower overall response are the resistivity of the bonding between the flexible PCB and the array, and the higher standard deviation of f_c for the flex transducers.

C. *Acoustical characteristics*

The acoustic characteristics of the flexible device are measured and compared with their rigid counterpart using the UMS-3 from Precision Acoustics. The transducer is attached to a holder and is submerged in a water tank. Square pulses from the Verasonics Vantage 64 are used to actuate the transducer between 1 and 4MHz. The acoustic response of the transducer is then measured using a 0.5mm Hydrophone from Precision acoustics placed 13cm away on the central axis. The distance is chosen to be at the peak of the natural focus distance of the device. The output of the hydrophone is then scaled in frequency domain based on its frequency dependent sensitivity calibration data and normalized to the peak drive voltage of 10V.

The measured and simulated frequency responses match very well suggesting a good model present to predict the behaviour of both flexible and rigid arrays. The peak Tx efficiency of the rigid transducer is 5kPa/V at a resonant frequency of 2MHz and the flexible device has a peak Tx efficiency of 3.8kPa/V at 1.8MHz. The frequency response shows that there is a reduction in the pressure and frequency of operation in the flexible device compared to its rigid counterpart from the same glass sheet. This is hypothesized to be due to the non-ideal mechanical anchoring for the pMUTs when they are placed on a flexible substrate over glass substrate. Furthermore, on a glass substrate there is a complete reflection of acoustic waves generated towards the backside of the pMUT membrane whereas with the flexible substrate, the acoustic impedance is closer to that of the Polyimide membrane material and therefore results in dissipation of backward propagated waves. This also contributes to a reduction in forward pressure. The effect of moving to a flexible substate over a rigid one results in a 25% reduction in peak transduction efficiency and a 10%

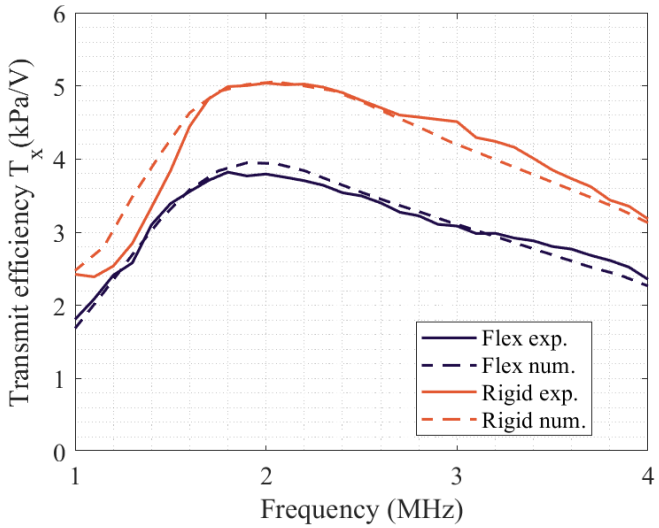

Fig. 7. Acoustic frequency response and transmission efficiency for rigid and flexible array of 32 rows by 32 columns of 4x4 PMUT pixels. The experimental data correlates well with the numerical simulation results.

reduction in resonant frequency. Since this effect can be predicted quite accurately by FEM, these changes can be taken into account in the design phase to hit the target specifications of the applications.

The results pave the way for flexible ultrasound patches being used for continuous monitoring of vital organs in a clinical setting. Next steps will be calibrating the beam steering for curved surfaces with the end goal of in-vitro and in-vivo trials on measuring cardiac or bladder volumes.

V. Conclusions

In summary, this work demonstrates the successful development of the first flexible micromachined ultrasound transducer (PMUT) array based on AlScN piezoelectric film, fabricated using flat-panel display compatible technology. The transition from rigid to flexible substrates, while resulting in a modest reduction in mechanical output and a 25% decrease in peak transduction efficiency, still enables predictable and controllable acoustic performance, as validated by both simulation and experimental results. The flexible 32×32 element PMUT arrays achieve a peak transmit sensitivity of 3.8 kPa/V at 1.8 MHz in water and maintain a high electromechanical coupling coefficient, paving the way for their integration into wearable and conformal devices.

Acknowledgment

This work was made possible through the “Listen2Future” project. Under grant 101096884, Listen2Future is co-funded by the EU and made possible with the support of VLAIO.

References

[1] W. Lee and Y. Roh, “Ultrasonic transducers for medical diagnostic imaging,” *Biomed Eng Lett*, vol. 7, no. 2, pp. 91–97, Mar. 2017.

[2] W. Manthey, N. Kroemer, and V. Magori, “Ultrasonic transducers and transducer arrays for applications in air,” *Meas. Sci. Technol.*, vol. 3, no. 3, p. 249, Mar. 1992.

[3] J. Joo, J. Koh, and H. Lee, “Hand Gesture Recognition Using Ultrasonic Array with Machine Learning,” *Sensors*, vol. 24, no. 20, p. 6763, Jan. 2024.

[4] C. Chare, P. Gijsenbergh, Y. Jeong, P. Heremans, J. Genoe, and D. Cheyns, “High performance large-area polymeric PMUT phased arrays in air,” in *2022 IEEE International Ultrasonics Symposium (IUS)*, Venice, Italy: IEEE, Oct. 2022, pp. 1–4. Accessed: Apr. 01,2025.

[5] P. Gijsenbergh, M. Billen, D. Wysocka, D. Cheyns, and V. Rochus, “Ultrasound Imaging in Mid-Air Using Phased Polymer PMUT Array,” in *2021 21st International Conference on Solid-State Sensors, Actuators and Microsystems (Transducers)*, Jun. 2021, pp. 62–65. Accessed: Aug. 29,2025.

[6] D. A. Horsley, O. Rozen, Y. Lu, S. Shelton, A. Guedes, R. Przybyla, *et al.*, “Piezoelectric micromachined ultrasonic transducers for human-machine interfaces and biometric sensing,” in *2015 IEEE SENSORS*, Nov. 2015, pp. 1–4. Accessed: Aug. 29,2025.

[7] K. Harrington, D. R. Large, G. Burnett, and O. Georgiou, “Exploring the Use of Mid-Air Ultrasonic Feedback to Enhance Automotive User Interfaces,” in *Proceedings of the 10th International Conference on Automotive User Interfaces and Interactive Vehicular Applications*, Toronto ON Canada: ACM, Sep. 2018, pp. 11–20. Accessed: Aug. 29,2025.

[8] T. Romanus, S. Frish, M. Maksymenko, W. Frier, L. Corenthy, and O. Georgiou, “Mid-Air Haptic Bio-Holograms in Mixed Reality,” in *2019 IEEE International Symposium on Mixed and Augmented Reality Adjunct (ISMAR-Adjunct)*, Beijing, China: IEEE, Oct. 2019, pp. 348–352. Accessed: Aug. 29,2025.

[9] X. Jiang, Y. Lu, H.-Y. Tang, J. M. Tsai, E. J. Ng, M. J. Daneman, *et al.*, “Monolithic ultrasound fingerprint sensor,” *Microsyst Nanoeng*, vol. 3, no. 1, p. 17059, Nov. 2017.

[10] A. T. Toymus, U. C. Yener, E. Bardakci, Ö. D. Temel, E. Koseoglu, D. Akcoren, *et al.*, “An integrated and flexible ultrasonic device for continuous bladder volume monitoring,” *Nat Commun*, vol. 15, no. 1, p. 7216, Aug. 2024.

[11] H. Hu, H. Huang, M. Li, X. Gao, L. Yin, R. Qi, *et al.*, “A wearable cardiac ultrasound imager,” *Nature*, vol. 613, no. 7945, pp. 667–675, Jan. 2023.

[12] Y. Jeong, J. Genoe, P. Gijsenbergh, J. Segers, P. L. Heremans, and D. Cheyns, “Fully Flexible PMUT Based on Polymer Materials and Stress Compensation by Adaptive Frequency Driving,” *J. Microelectromech. Syst.*, vol. 30, no. 1, pp. 137–143, Feb. 2021.

[13] C. Wang, B. Qi, M. Lin, Z. Zhang, M. Makihata, B. Liu, *et al.*, “Continuous monitoring of deep-tissue haemodynamics with stretchable ultrasonic phased arrays,” *Nat Biomed Eng*, vol. 5, no. 7, pp. 749–758, Jul. 2021.

[14] J. Elloian, J. Jadwiszczak, V. Arslan, J. D. Sherman, D. O. Kessler, and K. L. Shepard, “Flexible ultrasound transceiver array for non-invasive surface-conformable imaging enabled by geometric phase correction,” *Sci Rep*, vol. 12, no. 1, p. 16184, Sep. 2022.

[15] M. Pandit, J. Aerts, D. Barbosa, M. Forlin, P. Deruytere, E. Georgitzikis, *et al.*, “Developing a phased PMUT array patch for cardiac health monitoring,” in *2024 IEEE Ultrasonics, Ferroelectrics, and Frequency Control Joint Symposium (UFFC-JS)*, Taipei, Taiwan: IEEE, Sep. 2024, pp. 1–4. Accessed: Jun. 18,2025.

[16] E. Georgitzikis, P. Gijsenbergh, J. Segers, D. Wysocka, J. Viaene, T. Kuna, *et al.*, “78-2: A flat-panel-display compatible ultrasound platform,” *Symp Digest of Tech Papers*, vol. 54, no. 1, pp. 1101–1104, Jun. 2023.

[17] G. Massimino, F. Quaglia, A. Corigliano, and A. Frangi, “Model order reduction for the analysis of large arrays of piezoelectric micromachined ultrasonic transducers in water,” *Applied Acoustics*, vol. 182, p. 108231, Nov. 2021.

[18] G. Massimino, B. Lazarova, F. Quaglia, and A. Corigliano, “Air-coupled PMUTs array with residual stresses: experimental tests in the linear and non-linear dynamic regime,” *International Journal of Smart and Nano Materials*, vol. 11, no. 4, pp. 387–399, Oct. 2020.

[19] G. Massimino, A. Colombo, R. Ardito, F. Quaglia, and A. Corigliano, “Piezo-micro-ultrasound-transducers for air-coupled arrays: Modeling and experiments in the linear and non-linear regimes,” *Extreme Mechanics Letters*, vol. 40, p. 100968, Oct. 2020.

[20] G. G. Yaralioglu, A. S. Ergun, B. Bayram, E. Haeggstrom, and B. T. Khuri-Yakub, “Calculation and measurement of electromechanical coupling coefficient of capacitive micromachined ultrasonic transducers,” *IEEE Transactions on Ultrasonics, Ferroelectrics, and Frequency Control*, vol. 50, no. 4, pp. 449–456, Apr. 2003.